

The Effect of Solvent on the Ligand Substitution Reactions of Aquacobalamin (Vitamin B_{12a})

Leanne Knapton and Helder M. Marques*

Molecular Sciences Institute, School of Chemistry, University of the Witwatersrand, P.O. Wits, Johannesburg, 2050 South Africa.

Received 28 June 2005; revised 2 February 2006; accepted 29 April 2006.

ABSTRACT

The kinetics of the substitution of coordinated H₂O in aquacobalamin (H₂OCoBl⁺, vitamin B_{12a}) by pyridine (py) were studied as a function of temperature in water and in 70% (v/v) ethanol–water at pH 7.0. Saturation kinetics is observed, in agreement with a dissociative interchange mechanism. The values of ΔH^\ddagger for the rate constant for interchange of H₂O and py are 80(2) and 99(8) kJ mol⁻¹ in water and ethanol–water, respectively, while ΔS^\ddagger values are 47(8) and 106(27) J K⁻¹ mol⁻¹, respectively. There is a compensation effect between the two activation parameters which is interpreted in terms of the position of the transition state along the reaction coordinate. The transition state occurs later in an ethanol–water mixture, probably because the outer sphere complex that precedes the ligand exchange is less favoured than in pure water. Despite this compensation, the ligand substitution reaction is slower below about 50°C in the mixed-solvent system than in water. The present results, together with those previously reported by others, suggest that this may be a general feature of the ligand substitution reactions of H₂OCoBl⁺ in mixed solvents.

KEY WORDS

Vitamin B_{12a}, solvent effects, ligand substitution, inorganic reaction mechanisms.

1. Introduction

There is by now abundant evidence that the ligand substitution reactions of aquacobalamin (H₂OCoBl⁺, vitamin B_{12a}, Fig. 1, R = H₂O) in which the H₂O ligand coordinated to the upper (β) coordination site of Co(III) is replaced by an exogenous ligand, L, from solution proceeds through a dissociative interchange mechanism (I_d), which means that there is nucleophilic participation of L in the transition state (Scheme 1).^{1–9} Furthermore, even if the departing ligand is changed from H₂O to the much bulkier I⁻, the I_d mechanism persists.¹⁰

Less is known about the effect the solvent has on these reactions. Balt and co-workers investigated the reaction between H₂OCoBl⁺ and thiosulfate in a dioxane–water mixture,¹¹ thiourea in dioxane–water and acetonitrile–water,¹² and thiocyanate in acetonitrile–water.¹³ The rate of the reaction was found to decrease with the percentage of non-aqueous solvent in the solvent mixture. However, the effect was not large, with the second-order rate constant reported to decrease by at most an order of magnitude. It was therefore suggested that H₂OCoBl⁺ creates a chemical micro-environment around itself which is relatively insensitive to the bulk solvent. These workers discussed their kinetic results in terms of a dissociative mechanism (D), where there is unimolecular dissociation of water from Co(III) before the five-coordinate intermediate is captured by L),

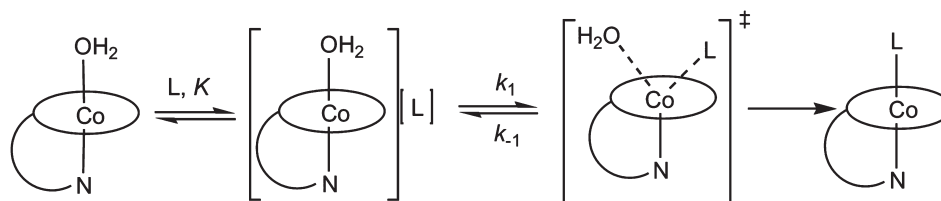
the prevailing view at the time^{14,15} although recognized, perhaps in acknowledgment of the view that a purely dissociative mechanism was improbable in aqueous solution,^{16,17} that their observations concerning the reaction between H₂OCoBl⁺ and thiosulfate in the dioxane–water mixtures are in agreement with both a D and an I_d mechanism.

For an I_d mechanism, when the observed pseudo-first-order rate constant, *k*, for replacement of H₂O by a ligand, L, is plotted against [L], *k* initially increases linearly with [L]. The gradient is the product of the equilibrium constant, *K*, for formation of the outer sphere complex, and the interchange rate constant, *k*₁ (Scheme 1). Thereafter *k* reaches a maximum saturating value (which may or may not be observable under experimental conditions, depending on the ligand L).¹⁸ This saturating value was originally interpreted as the rate of unimolecular dissociation of H₂O from H₂OCoBl⁺,¹⁸ but is now known^{7,9} to correspond to the interchange rate constant (*k*₁ in Scheme 1). We have undertaken an investigation of the reaction of H₂OCoBl⁺ with pyridine (py) in 70% (v/v) ethanol–water to determine the effect of the solvent on *K*, *k*₁ and *k*₋₁, and report on our findings in this paper.

2. Materials and Methods

All UV-vis spectra were recorded between 300 nm and 700 nm on a Cary 3E spectrophotometer, the cell compartment of which was thermostatted at 25.0°C ± 0.2°C by a water-circulating bath.

* To whom correspondence should be addressed.
E-mail: hmarques@aurum.chem.wits.ac.za



Scheme 1 Schematic representation of the ligand substitution reactions of aquacobalamin where substitution of axial H₂O by L proceeds through a dissociative interchange (I_d) mechanism after formation of an outer sphere complex.

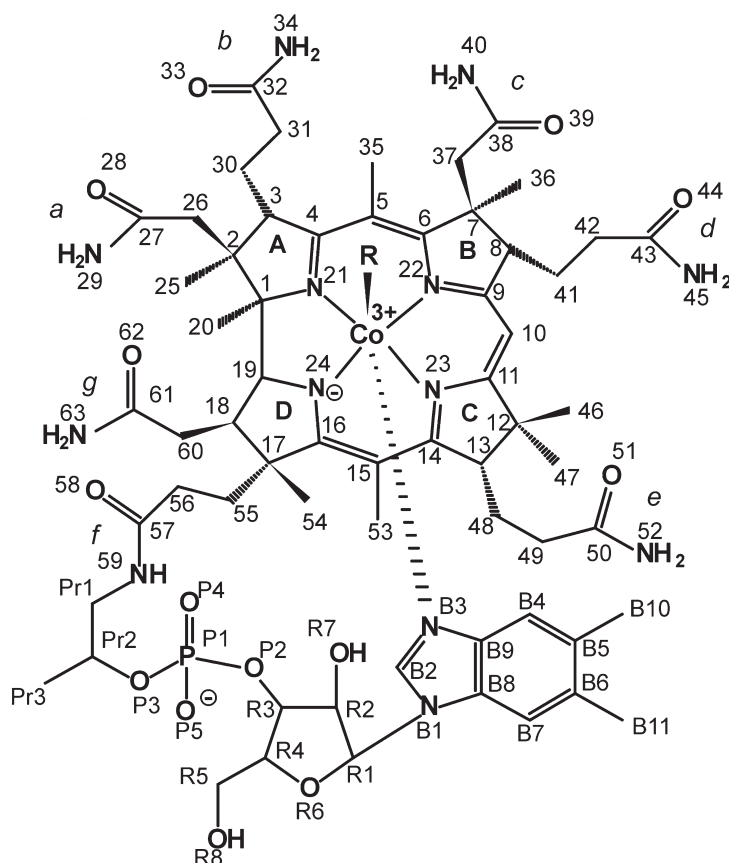


Figure 1 Standard view of the cobalamins (derivatives of vitamin B₁₂). In aquacobalamin (H₂OCo³⁺), R = H₂O.

Pyridine (BDH) was distilled before use. Hydroxocobalamin (>99% pure, HPLC) was from Roussel. Buffers were purchased from Sigma. Water was purified using a Millipore RO unit and further purified by passage through a Millipore MilliQ system (18 MΩ cm). The pH of all solutions was measured with a Metrohm 605 pH meter and a 6.02100.100 combination glass electrode calibrated against standard buffers, all maintained at the appropriate temperature with a water-circulating bath.

The acid dissociation constant of coordinated H₂O in H₂OCo³⁺, K_{Co} , was determined spectrophotometrically in a 2.00 cm pathlength cuvette at 522 nm. A solution (10 mL) with 25 μM H₂OCo³⁺, 10 mM MOPS (3-[N-morpholino]-propanesulfonic acid), 10 mM Tris/HNO₃ (tris[hydroxymethyl]aminomethane) and 10 mM CHES (2-[N-morpholino]-ethanesulfonic acid), and at a pH of approximately 6.5 was placed in a thermostatted glass cell and stirred; its pH was monitored with a glass electrode. The ionic strength was maintained at 0.1 M (NaNO₃). After the pH was measured, a peristaltic pump was used to transfer 2.5 mL of the solution into the cuvette in the cell-holder of the spectrometer. The solution was then transferred back to the glass cell where a capillary was used to add a tiny volume of concentrated NaOH solution. Once the glass electrode stabilized (the electrode response is slow in ethanol–water mixtures) the solution was again transferred to the cuvette and the absorbance measured at the monitoring wavelength. This procedure was repeated until a pH of 10.5 was reached. The experimental data were fitted to an ionization isotherm (Equation 1) as objective function using standard non-linear least squares methods employing a Newton-Raphson procedure, with A_p , the absorbance at the monitoring wavelength, K_a , the acid dissociation constant, A_0 , initial absorbance and A_1 , the final absorbance, as variables.

$$A_T = \frac{A_0}{1 + 10^{pH - pK_a}} + \frac{A_1}{1 + 10^{pK_a - pH}} \quad (1)$$

$$k = k_{obs}(1 + 10^{pH - pK_{Co}}) \quad (2)$$

The kinetics of all reactions were studied under pseudo-first-order conditions and monitored at 375 nm. Equal volumes (0.1 mL) of, firstly, a buffered (0.1 M MOPS, pH 7.0, ionic strength 0.1 M, NaNO₃) solution of between 50 and 80 μM H₂OCo³⁺ in water or in a 70% ethanol–water mixture and, secondly, a solution of pyridine, 0.2–2.0 M, also buffered at pH 6.5 and with the same ionic strength in the same solvent, were mixed in a Hi-Tech SF-51 stopped-flow spectrometer (cell pathlength 1.00 cm) interfaced through a DAS-50 A/D board with a computer. A water-circulating bath was used to maintain the temperature (±0.1°C) of the system. The reactions were monitored as a function of temperature. Pseudo-first-order rate constants, k_{obs} , were obtained by curve-fitting the absorbance-time trace to an equation of the form $A_1 \exp(-k_{obs}t) + A_2$, with A_1 , A_2 and k_{obs} as variables. At least six half-lives were monitored and fitted for each ligand concentration and these recorded traces were averaged to obtain the final k_{obs} value. Since hydroxocobalamin is inert to substitution,^{1,5} values of k_{obs} were converted into a pH-independent value, k , using Equation 2, where K_{Co} is the acid dissociation constant for coordinated H₂O in aquacobalamin. (As the acid dissociation constant of pyridine, 5.19,¹⁹ is very much lower than the operating pH, the fraction of protonated, and hence unavailable, ligand is insignificant.) Although the kinetics of the reaction of H₂OCo³⁺ and py in aqueous solution have been reported previously,^{18,20} we re-investigated this system to ensure that the results were obtained under identical conditions as those obtained in

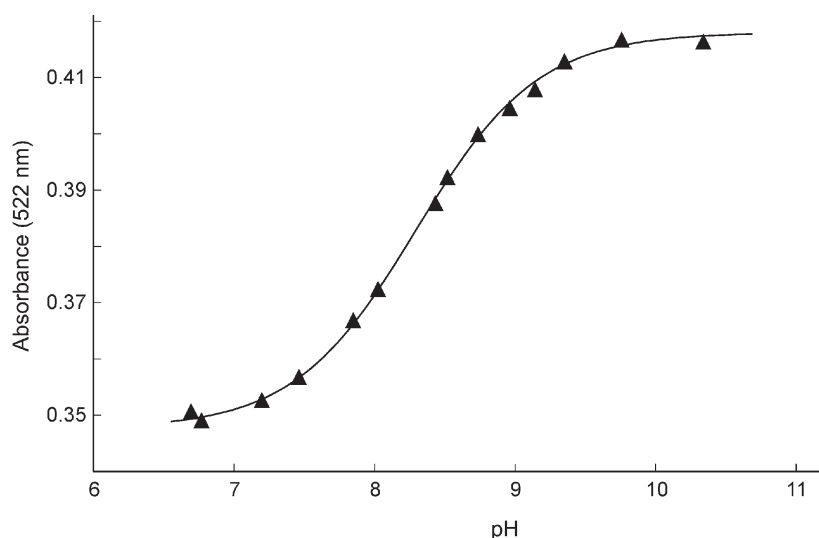


Figure 2 Spectrophotometric titration of H_2OCbl^+ in 70% (v/v) ethanol–water performed in a 2.00 cm pathlength cell at 25°C and monitored at 522 nm. The solid line is a non-linear least-squares fit of Equation 1 to the experimental data.

ethanol–water mixtures so that direct comparisons could be made.

3. Results and Discussion

The UV-vis spectrum in 70% ethanol–water is identical to that in pure water which strongly suggests that the coordination sphere of Co(III) is identical in the two solvents.

The titration of H_2OCbl^+ between pH 6.5 and 10.5 can be fitted to a single ionization isotherm (Fig. 2) attributed to ionization of coordinated H_2O with $\text{p}K_{\text{Co}} = 8.26 \pm 0.03$. There is therefore a small increase from the value in pure H_2O ($\text{p}K_{\text{Co}} = 8.09^1$; 8.11^{21}). The metal centre of hydroxocobalamin carries a +1 charge (–1 from the corrin and +3 from the metal; the negative charge on phosphate is some 9 Å away). It is therefore reasonable to expect that as the dielectric constant of the medium decreases on going from H_2O to 70% ethanol–water, the drive towards neutralization of large charge increases the basicity of coordinated OH^- . Because the effect is very small, this suggests that the immediate environment of Co(III) is very similar in the two solvents.

The dependence of the rate constant, k (Equation 2), on $[\text{py}]$ was studied as a function of temperature. It was immediately apparent that the reactions in ethanol–water were significantly slower than those in water. Moreover, while there was clear saturation of the values of k in water, the saturation in ethanol–water was less obvious. An example of the experimental data is shown in Fig. 3.

It has been shown⁸ that for an I_d mechanism the macroscopic pseudo-first-order rate constant, k , and the microscopic rate and equilibrium constants of Scheme 1 are related by Equation 3. For reliable fits of the experimental data to Equation 3 as objective function,

$$k = \frac{k_1 K [\text{L}]}{1 + K [\text{L}]} + k_{-1} \quad (3)$$

$$\frac{1}{k - k_{-1}} = \frac{1}{k_1 K [\text{L}]} + \frac{1}{k_{-1}} \quad (4)$$

significant saturation has to be observed because k_{-1} , the saturating rate constant, is a variable. As is seen in Fig. 3, saturating kinetics are not clearly attained in ethanol–water mixtures. Under these conditions, Equation 3 can be re-arranged to a linear form (Equation 4), and k_{-1} can be found from the intercept (which is $1/k_{-1}$) of a plot of $1/(k - k_{-1})$ against $1/[\text{L}]$; K can be found

from the gradient (which is $1/(k_1 K)$) once k_{-1} has been determined.

There are several drawbacks, however. Firstly, k_{-1} has to be known with a high degree of certainty, and any error in k_{-1} will have a significant effect on the data. Secondly, the problem with reciprocal plots is that the low ligand concentrations are heavily weighted and this can cause a significant skewing of the data. We addressed these problems by firstly using fits to Equation 3 in order to obtain the best possible value of k_{-1} , and then used this in Equation 4, but omitted the data for $[\text{py}] < 0.3 \text{ M}$. The results obtained are listed in Table 1. It will be noted that the results obtained from Equations 3 and 4 are virtually identical, within experimental error.

To determine the activation parameters ΔH^\ddagger and ΔS^\ddagger for k_1 and k_{-1} in water and in ethanol–water, $\ln(k_i h/k_b T)$, where $i = 1$ or -1 , h is the Planck constant, k_b is the Boltzman constant, was plotted against T^{-1} and the two parameters found from the gradient and intercept, respectively (Fig. 4). The values are listed in Table 2.

Values of K in water are small, but an order of magnitude larger than in ethanol–water (Table 1). A plot of $\ln K$ against T^{-1} gave reasonable straight lines (Fig. 5) from which $\Delta H = 13 \pm 4 \text{ kJ}$ and $\Delta S = 52 \pm 13 \text{ J K}^{-1} \text{ mol}^{-1}$ for the reaction in water, and $\Delta H = -32 \pm$

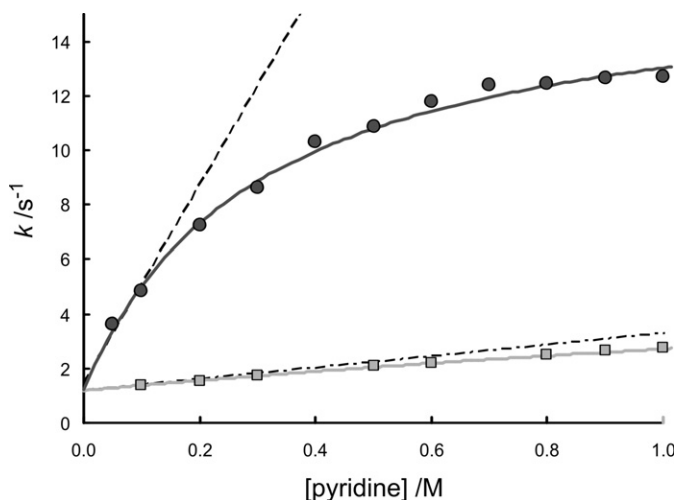


Figure 3 Dependence of the pseudo-first-order rate constant, k , for replacement of H_2O in H_2OCbl^+ by pyridine on pyridine concentration in (●) water and in (■) 70% (v/v) ethanol–water at 25°C, pH 7.0 (0.1 M MOPS). The solid lines are fits to Equation 3, while the broken lines are the limiting slopes at low $[\text{py}]$.

Table 1 Values of the interchange rate constant, k_i , the reverse rate constant, k_{-1} and the equilibrium constant for formation of the outer sphere complex for the reaction of pyridine and H_2OCbl^+ in water and in 70% ethanol–water (pH 7.0).

Solvent	Temp/°C	k_i/s^{-1} ^a	k_{-1}/s^{-1} ^a	$K/\text{dm}^3 \text{mol}^{-1}$ ^a	k_i/s^{-1} ^b	$K/\text{dm}^3 \text{mol}^{-1}$ ^b
Water	9.9	2.5(2)	0.17(5)	2.4(5)		
	15.0	4.4(1)	0.3(1)	3.1(5)		
	25.0	15.4(5)	1.2(5)	3.3(6)		
	29.9	24.4(6)	2.1(6)	3.6(4)		
70% Ethanol	5.0	0.54(9)	0.047(3)	0.30(7)	0.53(6)	0.31(4)
	15.0	3.0(7)	0.272(8)	0.28(6)	3.1(4)	0.27(2)
	25.0	7(2)	1.18(4)	0.18(10)	8(1)	0.16(4)
	35.0	77(52)	4.74(9)	0.07(5)	44(10)	0.13(3)

^a From Equation (3).^b From Equation (4) using the value of k_{-1} found from fits of Equation (3).**Table 2** Activation parameters for the reaction of pyridine with H_2OCbl^+ .

Solvent	$\Delta H^\ddagger/\text{kJ mol}^{-1}$	$\Delta S^\ddagger/\text{J K}^{-1} \text{mol}^{-1}$	$\Delta H^\ddagger/\text{kJ mol}^{-1}$	$\Delta S^\ddagger/\text{J K}^{-1} \text{mol}^{-1}$
	k_i		k_{-1}	
Water	80(2)	47(8)	89(3)	55(10)
70% Ethanol–water	99(8)	106(27)	107(2)	114(7)

4 kJ and $\Delta S = -121 \pm 12 \text{ J K}^{-1} \text{mol}^{-1}$ for the reaction in ethanol–water.

The values in Table 2 show that for this system, whether in water or in ethanol–water solvent, there is a compensation effect between ΔH^\ddagger and ΔS^\ddagger for both k_i and k_{-1} ; thus, the larger ΔH^\ddagger

and the less enthalpically favoured the reaction, the more positive ΔS^\ddagger and the more the reaction is entropically favoured. Since both the entering and the departing ligand are neutral, the effect cannot be due to electrostriction effects.

We have noted this compensation effect before in the ligand substitution reactions of the cobalt corrin.⁷ We interpret the effect to reflect the extent of the involvement of the incoming ligand in the transition state of the reaction. The later along the reaction coordinate the transition state occurs, the smaller the compensation for the breaking the Co– H_2O bond by formation of the Co–pyridine bond, and hence the larger ΔH^\ddagger ; however, this is offset by a smaller ΔS^\ddagger as the incoming ligand has greater freedom in the transition state. If this interpretation is correct, then we can conclude that the transition state occurs later in 70% ethanol–water than in water. This is probably a consequence of non-bonded (hydrophobic) interactions between pyridine and H_2OCbl^+ ; a tighter complex between the two is favoured in water than in ethanol–water (K is an order of magnitude larger, Table 1) and hence the ligand is able to participate in the transi-

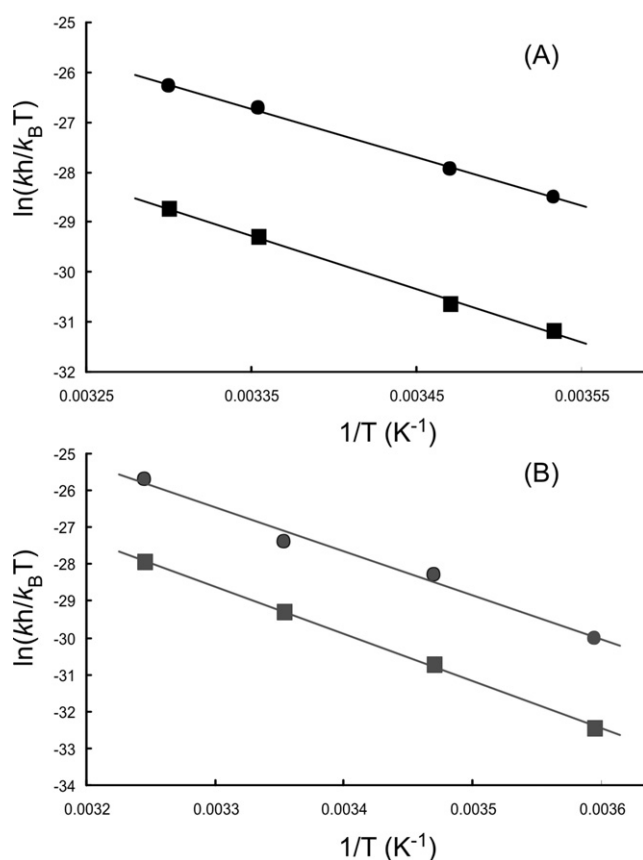


Figure 4 Plot of $\ln(kh/k_B T)$ against T^{-1} for the reaction of pyridine with H_2OCbl^+ in (A) water and (B) 70% ethanol–water, pH 7.0. The values are for k_i (●) and k_{-1} (■). The solid lines are linear least squares fits to the experimental data.

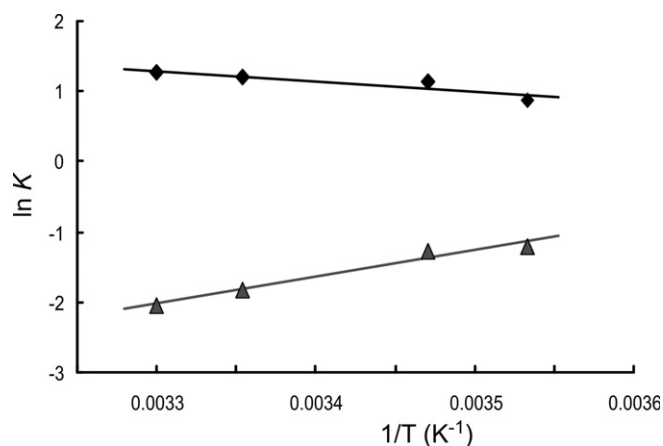


Figure 5 Plot of $\ln K$ against T^{-1} for the formation of the outer sphere complex between pyridine and H_2OCbl^+ in (◆) water and (▲) 70% ethanol–water, pH 7.0.

tion state earlier along the reaction coordinate.

The much higher ΔH^\ddagger value for k_1 in ethanol–water is not fully compensated near ambient temperature by an increase in ΔS^\ddagger ; the isokinetic temperature is near 50°C (the uncertainty in ΔH^\ddagger and ΔS^\ddagger preclude a more precise value) and at 25°C k_1 is smaller in the mixed solvent system than in water. This observation accords with the observations of Balt *et al.*^{12,13} The ligands they studied (thiourea, thiocyanate) did not show saturation kinetics and hence the rate constants they report are second-order rate constants, k_{11} . Such a rate constant is composite since $k_{11} = k_1K$ in an I_a mechanism. They found that for $L =$ thiourea in water and 70% acetonitrile–water, $k_{11} = 223$ and $122 \text{ M}^{-1} \text{ s}^{-1}$, respectively, at 25°C; in water and in 70% dioxane–water, $k_{11} = 214$ and $23 \text{ M}^{-1} \text{ s}^{-1}$, respectively. For $L = \text{SCN}^-$ in a water and 70% acetonitrile–water, $k_{11} = 3240$ and $1580 \text{ M}^{-1} \text{ s}^{-1}$, respectively. The analogous values for $L =$ pyridine at 25°C (i.e. values of k_1K) are 51 and $7 \text{ M}^{-1} \text{ s}^{-1}$ in water and 70% ethanol–water, respectively. It therefore appears that this phenomenon of the a marked decrease in the rate of ligand substitution of H_2OCbl^+ as the dielectric constant of the medium decreases is a general phenomenon that occurs with a variety of ligands (pyridine, thiourea, thiocyanate) in a variety of solvents (ethanol, acetonitrile, dioxane).

Acknowledgement

This work was made possible by funding from the National Research Foundations, Pretoria, and the University of the Witwatersrand.

References

- 1 H.M. Marques, K.L. Brown and D.W. Jacobsen, *J. Biol. Chem.*, 1988, **263**, 12378–12383.
- 2 H.M. Marques, T.J. Egan, J.H. Marsh, J.R. Mellor and O.Q. Munro, *Inorg. Chim. Acta*, 1989, **166**, 249–255.
- 3 H.M. Marques, *J. Chem. Soc., Dalton Trans.*, 1991, 339–341.
- 4 H.M. Marques, *J. Chem. Soc., Dalton Trans.*, 1991, 1437–1442.
- 5 H.M. Marques, E.L.J. Breet and F.F. Prinsloo, *J. Chem. Soc., Dalton Trans.*, 1991, 2941–2944.
- 6 H.M. Marques, *S. Afr. J. Chem.*, 1991, **44**, 114–117.
- 7 H.M. Marques, J.C. Bradley and L.A. Campbell, *J. Chem. Soc., Dalton Trans.*, 1992, 2019–2027.
- 8 H.M. Marques, O.Q. Munro, B.M. Cumming and C. de Nysschen, *J. Chem. Soc., Dalton Trans.*, 1994, 297–303.
- 9 M. Meier and R. van Eldik, *Inorg. Chem.*, 1993, **32**, 2635–2639.
- 10 H.M. Marques, L. Knapton, X. Zou and K.L. Brown, *J. Chem. Soc., Dalton Trans.*, 2002, 3195–3200.
- 11 S. Balt and A.M. van Herk, *Trans. Met. Chem.*, 1983, **8**, 152–154.
- 12 S. Balt, A.M. van Herk and W.E. Koolhaas, *Inorg. Chim. Acta*, 1984, **92**, 67–74.
- 13 S. Balt, M.W.G. de Bolster and A.M. van Herk, *Inorg. Chim. Acta*, 1985, **107**, 13–17.
- 14 D. Thusius, *J. Am. Chem. Soc.*, 1971, **93**, 2629–2635.
- 15 C. Poon, *Coord. Chem. Rev.*, 1973, **10**, 1–35.
- 16 W.C. Randall and R.A. Alberty, *Biochemistry*, 1966, **5**, 3189–3193.
- 17 W.W. Reenstra and W.P. Jencks, *J. Am. Chem. Soc.*, 1979, **101**, 5780–5791.
- 18 G. Stochel and R. van Eldik, *Inorg. Chem.*, 1990, **29**, 2075–2077.
- 19 H.H. Perkampus and G. Prescher, *Busenges. physik. Chem.*, 1968, **72**, 429–435.
- 20 L. Knapton and H.M. Marques, *J. Chem. Soc., Dalton Trans.*, 2005, 889–995.
- 21 L. Knapton, *Kinetic and Thermodynamic Studies of the Ligand Substitution Reactions of the Cobalamins*, Ph.D. thesis, University of the Witwatersrand, Johannesburg, 2005.